Neurobiology of Sleep and Circadian Rhythms 6 (2019) 35–43

Contents lists available at ScienceDirect

Neurobiology of Sleep and Circadian Rhythms

journal homepage: www.elsevier.com/locate/nbscr

Research paper

The neuron-specific interleukin-1 receptor accessory protein alters emergent network state properties *in Vitro*

Joseph T. Nguyen[a,1], Dinuka Sahabandu[c,1], Ping Taishi[a,1], Mengran Xue[c], Kathryn Jewett[b], Cheryl Dykstra-Aiello[a], Sandip Roy[c,2], James M. Krueger[a,2,*]

[a] Department of Integrative Physiology and Neuroscience, College of Veterinary Medicine, Washington State University Spokane, WA, USA
[b] Department of Genome Sciences, University of Washington. Seattle, WA, USA
[c] Department of Electrical Engineering, Washington State University, Pullman, WA, USA

ARTICLE INFO

Keywords:
Mice
Sleep
Delta wave power
Development
Neuronal/glial cultures
State emergence

ABSTRACT

Small *in vitro* neuronal/glial networks exhibit sleep-like states. Sleep regulatory substance interleukin-1β (IL1) signals via its type I receptor and a receptor accessory protein (AcP). AcP has a neuron-specific isoform called AcPb. After sleep deprivation, AcPb, but not AcP, upregulates in brain, and mice lacking AcPb lack sleep rebound. Herein we used action potentials (APs), AP burstiness, synchronization of electrical activity (SYN), and delta wave (0.5–3.75 Hz) power to characterize cortical culture network state. Homologous parameters are used *in vivo* to characterize sleep. Cortical cells from 1–2-day-old pups from AcP knockout (KO, lacking both AcP and AcPb), AcPb KO (lacking only AcPb), and wild type (WT) mice were cultured separately on multi-electrode arrays. Recordings of spontaneous activity were taken each day during days 4–14 *in vitro*. In addition, cultures were treated with IL1, or in separate experiments, stimulated electrically to determine evoked response potentials (ERPs). In AcP KO cells, the maturation of network properties accelerated compared to those from cells lacking only AcPb. In contrast, the lack of AcPb delayed spontaneous network emergence of sleep-linked properties. The addition of IL1 enhanced delta wave power in WT cells but not in AcP KO or AcPb KO cells. The ontology of electrically-induced ERPs was delayed in AcP KO cells. We conclude IL1 signaling has a critical role in the emergence of sleep-linked network behavior with AcP playing a dominant role in the slowing of development while AcPb enhances development rates of sleep-linked emergent network properties.

1. Introduction

Sleep profoundly impacts almost all neurobiological processes. Yet, consensus is lacking as to the minimal neuronal/glial network required for the emergence of sleep states and whether molecular mechanisms responsible for organism sleep also operate at a local level to influence sleep-like states. A common finding of all brain lesion studies, whether due to stroke or experimental lesions, is that after damage to any brain area, including the sleep regulatory circuits, if the animal or human survives, sleep always ensues. Such findings indicate no specific brain area is necessary for sleep to manifest. Further, recent evidence indicates that sleep is a self-organizing emergent neuronal/glial network property of any viable network regardless of size or location whether *in vivo* or *in vitro* (Krueger et al., 2013; Krueger and Obál, 1993; Krueger et al., 2008; Rector et al., 2005; Roy et al., 2008). To determine when a subject, or small network, is asleep, two or more physiological variables that change with sleep/wake states are needed (Krueger et al., 2016). Common measures used to characterize sleep *in vivo* include: the electroencephalogram (EEG), EEG delta wave (0.25–3.75 Hz) synchronization (SYN), EEG delta wave power and evoked response potentials (ERPs). These *in vivo* measures are greater during non-rapid eye movement sleep (NREMS) than during waking.

In vitro neuronal/glial cultures are simple in comparison to whole brains, yet the cultures exhibit homologous electrical properties to those used to characterize sleep *in vivo* (Corner, 2008; Hinard et al., 2012; Jewett et al., 2015). These properties spontaneously emerge as networks mature and are influenced by stimulations that similarly affect whole animal brain states. For example, spontaneous culture delta wave power emerges several days after action potentials are present (Jewett et al., 2015). With appropriate stimuli, such cultures transition

* Correspondence to: P.O. Box 1495 Spokane, WA 99210-1495, USA.
E-mail address: J.Krueger@wsu.edu (J.M. Krueger).
[1] Equal contributions.
[2] Equal senior author contributions.

https://doi.org/10.1016/j.nbscr.2019.01.002
Received 6 December 2018; Received in revised form 3 January 2019; Accepted 14 January 2019
Available online 18 January 2019

into a more wake-like state or deeper sleep-like state depending upon the specific stimuli (Corner, 2008; Hinard et al., 2012; Wagenaar et al., 2005). Further, after an electrical stimulus-induced (Jewett et al., 2015), or after excitatory neurotransmitter treatment-induced (Saberi-Moghadam et al., 2018) wake-like period, the spontaneous sleep-like state is more intense the next day indicating rebound sleep homeostasis occurs *in vitro*. Collectively these results suggest that the electrophysiological measures used to define *in vivo* sleep also are useful to define *in vitro* states. Herein we extend these *in vitro* observations to show that sleep-like states in mixed cultures of neurons and glia are dependent in part on the interleukin-1 receptor accessory protein (AcP).

Interleukin-1β (IL1) is a well-characterized sleep regulatory substance (Imeri and Opp, 2009; Jewett and Krueger, 2012; Krueger et al., 1984). For instance, when injected, it induces excess NREMS including delta wave power enhancement (Krueger et al., 1984). IL1 also plays a role in sleep responses to inflammatory challenges (Davis et al., 2015; Garlanda et al., 2013; Taishi et al., 2012). In brain, IL1 has several additional functions, including being involved in synaptogenesis (Yoshida et al., 2012), synaptic activity (Gruber-Schoffnegger et al., 2013; Kawasaki et al., 2008; Gardoni et al., 2011; De et al., 2002), and cortical neuron migration (Ma et al., 2014). Low physiological amounts of IL1 enhance, while high pathological amounts of IL1 inhibit sleep (Opp et al., 1991), learning, memory, long-term potentiation (Bellinger et al.,1993; Katsuki et al., 1990; Yirmiya and Goshen 2011), and stress responses (Goshen and Yirmiya, 2009).

IL1 signaling requires the presence of AcP (Boraschi and Tagliabue, 2013; Dinarello, 2009; Garlanda et al., 2013; Cullinan et al., 1998). In brain, there is an AcP isoform, neuron-specific AcPb (Huang et al., 2011; Smith et al., 2009). AcPb mRNA, but not AcP mRNA, increases with sleep loss (Taishi et al., 2012). Mice lacking AcPb have exaggerated sleep responses after lipopolysaccharide administration (Taishi et al., 2012). AcPb is anti-inflammatory (Prieto et al., 2015) whereas AcP is pro-inflammatory (Smith et al., 2009). After sleep deprivation, mice lacking AcPb lack a homeostatic NREMS rebound (Davis et al., 2015). Herein, we demonstrate that *in vitro* cells from AcPb knockout (KO) mice develop the sleep-characterizing emergent electrophysiological properties, burstiness, SW SYN, and delta wave power more slowly than WT cells. In contrast, if cells from AcP KO mice, which lack AcP and AcPb isoforms, are used, maturation of these measures is accelerated. Further, cells lacking AcP and/or AcPb have distinct responses to IL1. Finally, we show that electrical-induced ERPs increase in amplitude and slow wave (SW) content over the course of cultured neural network development. We conclude that AcP/AcPb are important determinants for small network emergence of sleep-linked electrophysiological parameters. Current results also support the hypothesis that sleep is a fundamental property of small networks (Krueger and Obál, 1993).

2. Materials and methods

2.1. Culture preparation and maintenance

C57BL/6J (wild type; WT), AcPb KO and AcP KO mice were purchased from Jackson Labs (Bar Harbor, ME, USA) under the auspices of an agreement with Amgen, Inc (Thousand Oaks, CA). Homozygotic mice were bred 2–6 generations at Washington State University (WSU). Animal procedures were approved by the WSU Institutional Animal Care and Use Committee and complied with NIH guidelines. Mice were kept in a separate breeding room at 24 ± 2 °C, 40% humidity ± 10% on a 14 h light, 10 h dark schedule, lights on at Zeitgeber time 0 (ZT0). Cortical cells were harvested in the morning (ZT3 ± 1 h) from 1- or 2-day old pups and seeded onto 6-well multi-electrode arrays (MEAs; Multi Channel Systems, Reutlingen, Germany) as previously described (Jewett et al., 2015). Cortical tissues were initially placed in ice-cold Hibernate-E (HE, BrainBits, Springfield, IL) then digested with 2 mg/mL of papain (LS003119, Worthington Biomedical, Lakewood, NJ) for 20 min at 37 °C. Tissues were dispersed by trituration in HE with 2% GlutaMAX (35050-061, Invitrogen, Grand Island, NY) by passing the tissue through a 20-gauge needle and syringe twice, then again using a 22-gauge needle once. The tissue/cell suspension was passed through a 40 μm strainer to remove aggregated cells. Cells were then centrifuged at 200*g* for 10 min at room temperature. The precipitate was dissolved in warm Dulbecco's Modified Eagle Serum (DMEM; D6429, Sigma, St. Louis, MO) with 10% fetal bovine serum (FBS), 1% GlutaMAX, and 2% penicillin/streptomycin (pen-strep). Cells were counted using a hemocytometer and then plated (2×10^5 cells/20 μL) in each of the six individual MEA wells. Wells were pre-coated with poly-D-lysine (P6407, Sigma) solution for 1 h, rinsed three times with deionized water, and dried for 1 h prior to the introduction of cells.

The cells were then incubated in a 5% CO_2 humidified incubator at 37 °C for 50 min and then given 350 μL/well of warm DMEM/FBS/GlutaMAX/pen-strep media. After 4 h, 350 μL of NbActiv4 (Nb4–100, BrainBits; includes a mitotic inhibitor to suppress glial proliferation), 2% pen-strep, 0.2% Gentamycin (15710-064, Invitrogen) media was added to each well. MEAs were covered with Teflon membranes (ALA Scientific, Farmingdale, NY) to prevent water loss throughout the experiments. Half of the media was removed and replaced with fresh NbActiv4/pen-strep/Gentamycin solution every 3 to 4 days. Cultured cells on the MEAs were kept in a 5% CO_2 humidified incubator at 37 °C when not being recorded from.

2.2. MEA recordings

A MEA60-BC system from Multi Channel Systems was used to record from cells in a dry incubator at 37 °C and 5% CO_2. The MEA1060-Inv-BC system used has 60 electrodes distributed in 6 independent wells. Each well contains 1 silicon nitride substrate-integrated reference electrode and 9 titanium nitride electrodes in a 3 × 3 grid arrangement spaced 200 μm apart. The voltage at each individual electrode relative to its respective ground electrode was recorded at a sampling rate of 10 kHz. Raw data from recordings were stored on the acquisition computer and later transferred to external hard drives until analyzed.

2.3. MEA data analyses of spontaneous electrical activity during development

Six measurements were calculated: action potentials per second (APs/s), the percent of electrodes with greater than 0.5 APs/s, the number of bursts/min, a burstiness index (BI), SW SYN, and SW power as previously described (Jewett et al., 2015). MC_Rack software (Multi Channel Systems) was used for extraction of APs. After passing the raw signal through a 200 Hz high pass second-order Butterworth filter, the mean voltage ± 4 standard deviations (SD) from a 500 μs time interval was used to set limits for counting APs. Thus, any electrical activity exceeding the ± 4 SD threshold was counted as an AP.

Bursts were defined as a minimum of 4 APs within the first 10 ms with no more than 10 ms between APs within a burst, a minimum burst duration of 20 ms and a minimum of 10 ms between individual bursts. The BI was quantified by dividing 5 min recordings into 300 - 1 s long epochs, counting the number of APs in each epoch, and then the number of APs in the top 15% of the 300 epochs was divided by the total number of APs occurring in the 5 min interval (# of APs in top 15% [45 epochs])/# of total APs across all 300 epochs (Wagenaar et al., 2005). Random firing is associated with lower BI while a higher BI designates greater burstiness.

SW activity, low-pass (100 Hz) and high-pass (0.1 Hz) contents were extracted using second-order Butterworth filters; data were sampled at 100 Hz. Fast-Fourier transform (FFT) spectra from signals at randomly sampled active network nodes were calculated using a custom MATLAB program for 30 min periods across development days, or other time blocks in different experiments, using a cosine-tapered window. Spectral content for the 0.25–30.25 Hz range was binned into 0.5 Hz

frequency bands then summed from 0.25–3.75 Hz to obtain delta power.

SW SYN values between each set of adjacent channels were determined using the following equation:

$$\frac{\sum (V_1(t) - \bar{V}_1)(V_2(t) - \bar{V}_2)}{\sigma v_1 \sigma v_2}$$

Where $V_1(t)$ and $V_2(t)$ are the voltages at two different electrodes within a MEA well at time t, $\bar{V}_1$ and $\bar{V}_2$ are the sample means, and σv_1 and σv_2 are the standard deviations of the samples. The paired SW SYN values were averaged to produce a single SYN value for each MEA well. High SYN values indicate a high SW synchrony between electrodes while low SYN values represent low SW synchrony; values range from -1 to $+1$.

2.4. Experiment 1: Development of spontaneous activity

Neuronal activity development *in vitro* was characterized using seven independent cortical cell preparations. Cells were plated on 13 six-well MEAs. MEAs were microscopically examined to confirm cells were present in each well. Recordings were obtained from each MEA on each day for 1 h, starting after 4 days in culture and then repeated each culture day until day 14. MEAs were plated with WT cells in wells 1–3 or 4–6, and the remaining wells contained either AcPb KO or AcP KO cells. There were 3 MEAs with only AcP KO cells due to lack of WT cell availability. Each electrode was treated as an independent sample because the different spatial distribution of cells around each electrode varied over the 15-day development period. Thus, each electrode had its own unique pattern of electrical output. Data from 27 wells and 240 electrodes were used to calculate emergent electrical properties for WT cells. AcPb KO cell data were analyzed from 18 wells and 162 electrodes. Lastly, AcP KO cell data were analyzed from 33 wells and 297 electrodes. During the first 30 min of recording after transfer of MEA to the recording system, APs/s values decreased exponentially. Thus, only the last 30 min of the 1 h recordings were used as baseline data for data analyses. Means and SEMs were calculated from the aggregate data and graphically displayed according to cell type. No data were excluded from the statistical analyses of development data except for omitting electrode # 47 from 3 MEAs containing WT cells on one occasion because the specific head pin was not working properly. Statistical significance between strain and time (days) was determined using a two-way ANOVA (time and strain). If main effects were found, a post hoc, Fischer's least significant difference test was used to evaluate strain and time combinations.

2.5. Experiment 2: IL1 differentially affects network emergent properties

IL1 was added to cultures during development day 14 or 15 *in vitro*. MEAs were plated in the same manner as the development experiments with half the wells containing WT cells and the other half with either AcPb KO or AcP KO cells. After a 1 h baseline recording, 0.0 ng (control), 0.01 ng, or 0.1 ng of IL1 dissolved in 5 μL of saline was added to designated wells of each MEA. Recording promptly resumed following the addition of IL1. Data collected were used to calculate APs/sec, BI, SYN, and delta power as described for Experiment 1 and in Fig. 2 legend. These values were calculated for the first 5–10 min time block after IL1 additions to avoid artifacts associated with removal of the Teflon MEA cover and the addition of fluid to the cell media.

Data from 18 MEAs (7 preparations, 83 wells, 729 electrodes) were used to analyze the effects of IL1 on network properties. Wells with average baseline values of 1 AP/sec or more were included in the data analyses; an average of 1 AP/sec or greater was interpreted as an indicator of a healthy culture. Further, electrodes from those wells with values of less than 0.25 APs were excluded because APs/sec recorded from MEAs containing media but not cells have noise values of about 0.25 APs/s. In addition, electrodes that did not fall within ± 2 SD calculated from individual well values were also removed. All other data from included electrodes, whether treated with IL1 or saline were used in the data analyses. One-way ANOVAs (dose) were used to determine if there were main effects within each strain. If main effects were found, a post hoc, Fischer's least significant difference test was used to determine if there were significant differences between specific doses.

2.6. Experiment 3: Development of electrical evoked response potential

To better understand how AcPb and AcP affect emergent neuronal network properties, we also characterized the development of the responses to electrical stimulation using WT, AcPb KO, and AcP KO cells. Biphasic voltage (duration 200 μs and amplitude 600 mV) was applied at one electrode in each well. Similar to Experiment 1, cells were plated on 6 six-well MEAs: wells 1–3 of three MEAs contained WT cells and wells 4–6 contained AcPb KO cells; the remaining three MEAs contained AcP KO cells in all six wells. On development days 5, 10, and 14, an electrical stimulation was applied at one electrode in each well every 10 s (0.1 Hz stimulation frequency), for a 30 min period. The ERP was defined as the voltage signals measured at the non-stimulated electrodes between 0.1 s and 9.1 s after each stimulation; each stimulation cycle is 10 s in duration and ERPs return to baseline levels within the 9 s analysis period (Fig. 4). Data from 5 to 30 min after the initiation of stimulation were analyzed. Data from the first 5 min were ignored to avoid possible stimulus artifacts.

2.7. MEA data analyses of electrical evoked responses during development

For each ERP, two metrics were defined. First, the peak-to-peak voltage was defined as the difference between the evoked potential maximum voltage and minimum voltage (i.e. during 0.1 s to 9.1 s after each stimulation) (Fig. 4). Second, the slow-wave power was defined as the total evoked response frequency content between 0.25 and 1 Hz. To find the slow-wave power, an FFT was found for the evoked response signal, and the amplitudes of the FFT corresponding to the frequencies within the 0.25–1 Hz band were summed. The slow-wave power is presented on a decibel scale. The mean peak-to-peak value and slow-wave power were determined for each development day and cell type averaged over all wells, all electrodes, and all stimulation periods. The fractions of the evoked potential signals for which each metric exceeded a threshold of peak to peak 10 mV, and 80 dB for slow-wave power, were determined. Further, for each of these computations, the standard errors were computed. Each well was treated as an independent experiment (9 wells for WT, 9 wells for AcPb KO, and 18 wells for AcP KO).

3. Results

3.1. Experiment 1: emergent spontaneous network properties

To determine whether the absence of AcP and AcPb, or only AcPb, altered the time courses of emergent network properties we compared the *in vitro* ontology of six emergent network properties obtained from WT, AcPb KO and AcP KO cells. The choice of measurements was derived from the literature (Corner, 2008; Hinard et al., 2012; Jewett et al., 2015; Wagenaar et al., 2005; Jimbo et al., 1998). The focus of our interests was on those properties for which there are homologs in live animals and which are used to characterize sleep. These include number of APs, burstiness, SYN, and delta wave power. The general conclusions are that the absence of AcP and AcPb, or AcPb alone, affected the rate of emergence of all the properties determined. Another broad finding was that without AcPb, network activity developed very slowly regardless of the parameter determined.

Spontaneous APs/sec are perhaps the most fundamental indication of cell and network development (Fig. 1). Few APs occurred during day

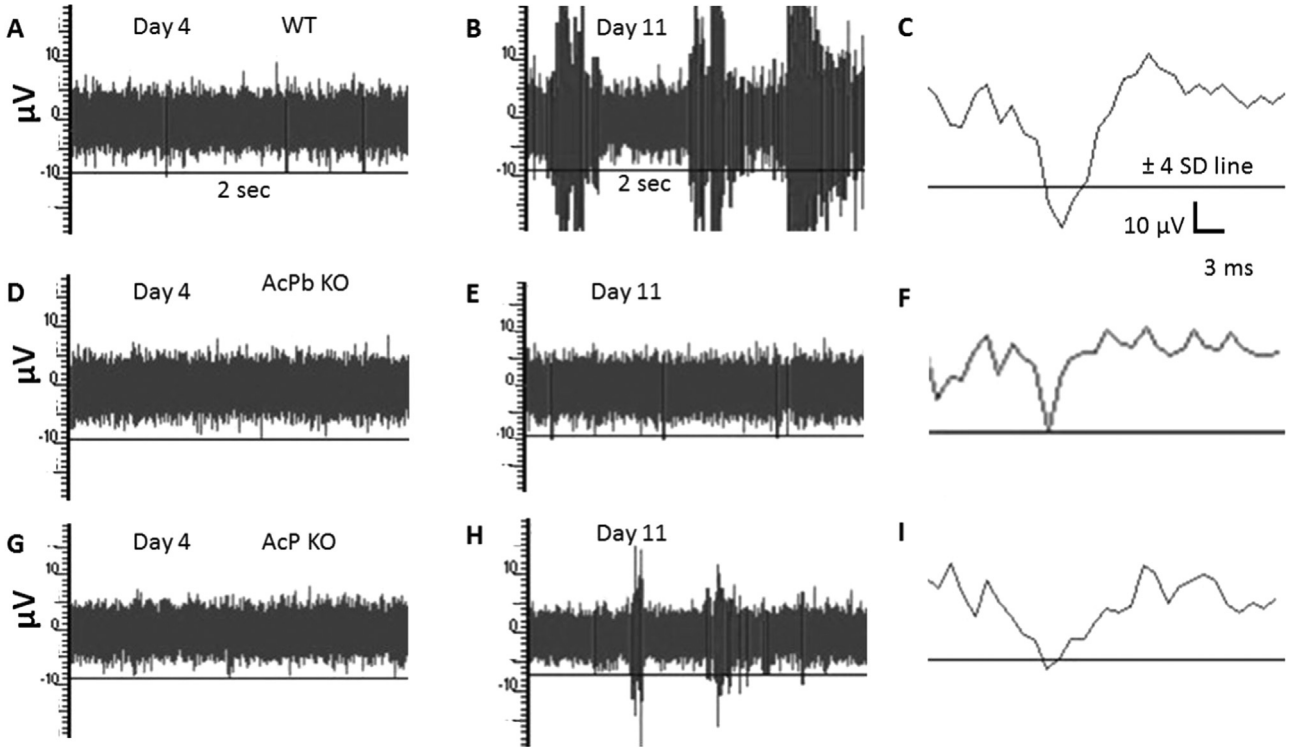

Fig. 1. A, B, D, E, G, and H are representative of single-channel raw data using a 200 Hz high-pass filter on days 4 and 11 *in vitro*. C, F, and I show single action potentials (AP). The solid horizontal lines are the -4 standard deviation lines from the baseline averages on day 11 derived from the specific electrode illustrated. If measured voltage was equal to or greater than the – or + 4 SD, the event was counted as an AP.

4 compared to day 11 in culture regardless of the mouse strain source of the cells. By day 11 greater AP activity was evident and the extracellular APs recorded had the expected voltage/time profile (Fig. 1 E,F, I). Two-way ANOVA analyses indicated main effects for time and strain (time - $F_{(10,\ 6,794)} = 75.51$, $p < 0.01$; strain - $F_{(2,\ 6,794)} = 52.46$, $p < 0.01$), there is also an interactive effect between time and strain (time x strain - $F_{(20,\ 6,794)} = 10.73$, $p < 0.01$) (Fig. 2A). In WT cells, APs/sec were relatively modest during the first 8 days in culture. By day 9, significant increases in APs/sec occurred in WT cells compared to their values on day 4 (day 9 vs day 4; $p < 0.01$). In AcPb KO and AcP KO cells, significant increases in APs/sec did not occur until day 11 (day 11 vs day 4 for AcPb KO $p = 0.03$; for AcP KO, $p < 0.01$). From days 10–14 APs/sec were highest in WT cells followed by AcP KO cells and lowest in AcPb KO cells. Although APs/sec remained higher than the baseline day 4 values after day 9, and statistical differences between strains were evident on day 14, spontaneous APs/sec values from the 3 strains converged on day 14. In prior studies, similar APs/sec development curves obtained from WT cells were reported (Hinard et al., 2012; Jewett et al., 2015).

Within the MEA literature, often only electrodes having greater than 0.5 APs/sec are used for data analyses. Thus, for each MEA well we determined the fraction of electrodes having greater than 0.5 APs/sec (Fig. 2B); 2-way ANOVA indicated main effects for time and strain (time - $F_{(10,\ 820)} = 26.69$, $p < 0.01$; strain - $F_{(2,\ 820)} = 16.31$, $p < 0.01$), and also an interactive effect between time and strain (time x strain - $F_{(20,\ 820)} = 2.31$, $p < 0.01$). Although these values for AcPb KO cells on day 4 were higher than those from WT or AcP KO cells, only modest increases occurred in AcPb KO cells over the subsequent 10 days. From days 9–13 there were significant differences between the strains with AcP KO cells having the greatest values, followed by WT cells, with AcPb KO cells having the lowest values. As with APs/sec, there was a convergence of values obtained from the 3 strains on day 14 although WT values remained significantly different from the other two cell types.

The number of bursts/min also changed over the initial 14 days in culture and 2-way ANOVA indicated time and strain main effects (time - $F_{(10,\ 7,095)} = 123.95$, $p < 0.01$; strain - $F_{(2,\ 7,095)} = 29.60$, $p < 0.01$), and an interactive effect between time and strain (time x strain - $F_{(20,\ 7,095)} = 7.74$, $p < 0.01$). The bursts/min values (Fig. 2C) paralleled APs/sec values (Fig. 2A). In WT cells, bursts/min on day 9 became significantly higher than their corresponding values on day 4 ($p < 0.00001$) and that value from WT cells was higher than day 9 values obtained from AcP KO and AcPb KO cells. By day 11, cells from all three strains exhibited more bursts/min than they did on day 4. All 3 strains exhibited large increases from day 10 to day 11 in their number of bursts. As with the other measures thus far presented, values from the 3 strains of cells converged on day 14, although some small differences remained significantly different.

The BI (Fig. 2D) provides a more nuanced view of the structure of AP bursts as BI values reflect the fraction of APs found within bursts. Two-way ANOVA analysis indicated main time and strain effects (time - $F_{(10,\ 7,036)} = 128.4$, $p < 0.01$; strain - $F_{(2,\ 7,036)} = 26.30$, $p < 0.01$), and an interactive effect between time and strain (time x strain - $F_{(20,\ 7,036)} = 5.0$, $p < 0.01$). By day 9 in culture, cells from all 3 strains had BI increases. From day 9 to day 14 the BI values stayed relatively flat and there were strain differences on all these days. Thus, the increases in APs/sec occurring after day 10 seemed to be absorbed within bursts while the number of bursts increased as well in parallel. This suggests that the cells within the *in vitro* circuits were gaining the ability to excite each other, thereby producing more bursts. Unlike the previous 3 measurements presented, the BI did not show evidence of convergence on day 14, yet although relative differences in the BI between the 3 strains were small, they were significant.

Synchrony of voltages between adjacent electrodes (SYN values) were clearly different in cells from the 3 strains across recording days (Fig. 2E). Two-way ANOVA analysis indicated time and strain main effects (time - $F_{(10,\ 15,979)} = 415.13$, $p < 0.01$; strain - $F_{(2,\ 15,979)} = 2080.43$, $p < 0.01$), and an interactive effect between time and

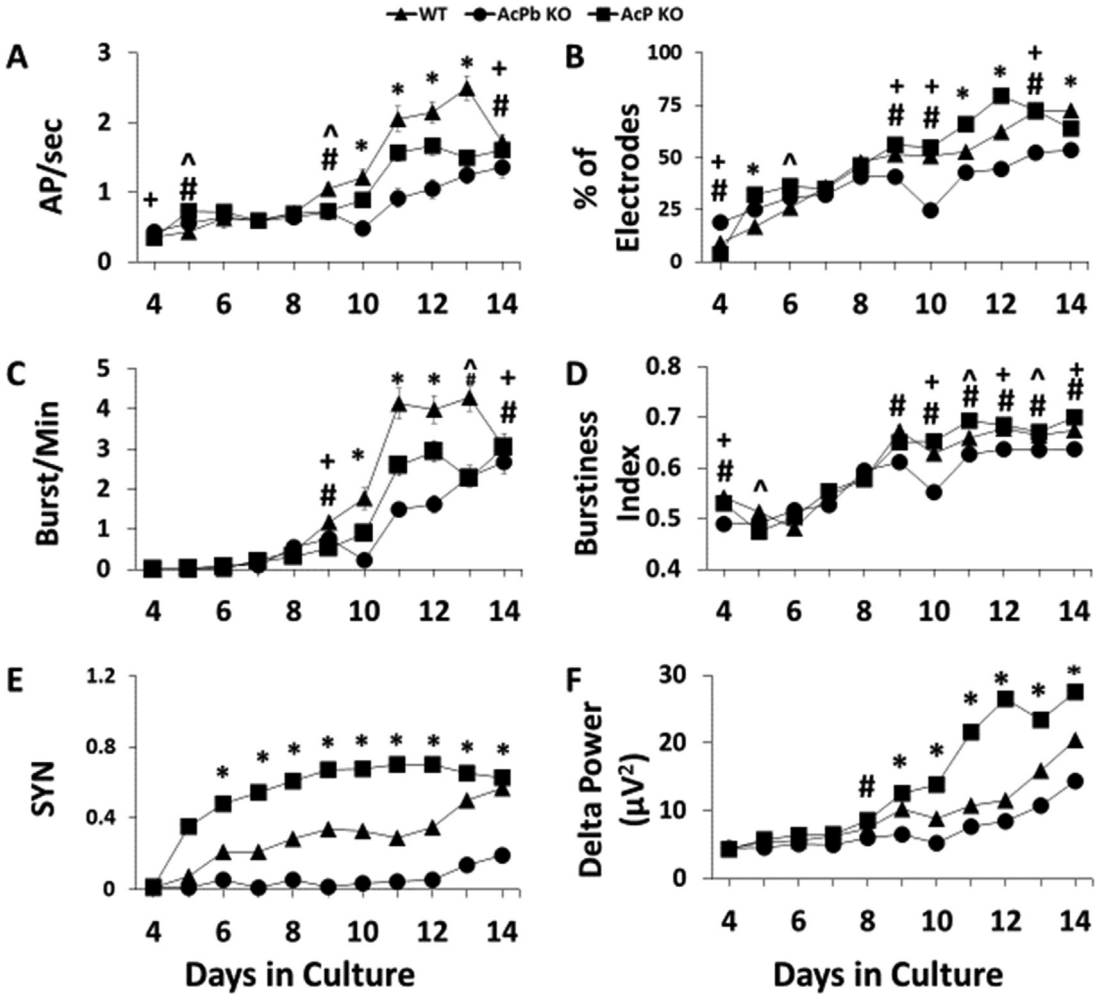

Fig. 2. Development of spontaneous electrical activity in co-cultures of cortical neurons and glia derived from C57BL6 (WT), AcP KO, and AcPb KO mice (WT, 3 preparations, 9 MEAs, 27 wells, and 240 electrodes; AcP KO, 2 preparations, 7 MEAs, 33 wells, and 297 electrodes; AcPb KO, 2 preparations, 6 MEAs, 18 wells, and 162 electrodes). Means and ± SEM from days 4–14 in culture are shown. (A) Average values for action potentials/sec (APs/s) occurring each day during development for each strain are shown. (B) Electrodes with > 0.5 APs/s were counted for each well and divided by the total number of well electrodes. The percent of electrodes from each well having > 0.5 APs/s were averaged to get the values shown. (C) Mean number of bursts/min. (D) Mean burstiness index (BI). (E) Average SYN values between adjacent electrodes. (F) Mean fast Fourier transformation values (delta wave power; μV^2) within the 0.25–3.75 Hz frequency band values are shown. SEMs are not evident at many points because they are contained within the data points. (* = WT vs AcP KO vs AcPb KO, $P < 0.01$; # = AcP KO vs AcPb KO, $P < 0.01$; + = WT vs AcPb KO, $P < 0.01$; ^ = WT vs AcP KO, $P < 0.01$).

strain (time x strain - $F_{(20,\ 15,979)} = 37.77$, $p < 0.01$). Even on day 5, AcP KO cells had higher SYN values than they did on day 4 (between day 4 and 5 for AcP KO, $p < 0.01$) and those higher values persisted through day 14. In contrast, SYN values from WT cells were not significantly different from their day 4 values until day 6 while SYN values from AcPb KO cells were not above their day 4 values until day 13. From day 5 through day 14, SYN values were highest in AcP KO cells with WT cells having intermediate SYN values and AcPb KO cells with the lowest values. As mentioned in prior work (Jewett et al., 2015), SYN values have an *in vivo* homolog used to characterize sleep with higher values indicating more sleep-like electrical activity.

Delta wave power was determined from the filtered (0.25–3.75 Hz) component of recordings using FFT. This measure is obtained and analyzed using the same methods as with EEG recordings from live animals. Delta wave power is often used as the determining indicator of NREMS (Davis et al., 2011). Delta wave power had time and strain main effects as determined from two-way ANOVA (time - $F_{(10,\ 6,873)} = 177.07$, $p < 0.01$; strain - $F_{(2,\ 6,873)} = 283.53$, $p < 0.01$), and an interactive effect between time and strain (time x strain - $F_{(20,\ 6,873)} = 26.12$, $p < 0.01$) . By day 8, delta wave power values from AcP KO cells were higher than corresponding values obtained from these cells on day 4 (AcP KO, $p = 6.65 \times 10^{-4}$). Also, by day 8, values from AcP KO cells were higher than those from WT and AcPb KO cells (Fig. 2F). From day 8 through day 14 delta wave power values from AcP KO cells remained greater than those from WT cells which were greater than those from AcPb KO cells. There was no evidence of convergence of delta wave power values from the 3 strains of cells on day 14 as observed in most of the other measures presented in Fig. 2. The development of WT mice delta wave power *in vivo* parallels that observed *in vitro*, and previously described (Jewett et al., 2015).

3.2. Experiment 2: Effects of IL1 on mature WT, AcPb KO, and AcP KO cells

To determine the effects of IL1 on APs/s, BI, SYN, and delta wave power, various amounts of IL1 (0.0, 0.01, and 0.10 ng)(11.8 pM final high dose concentration) were added on d14 or d15 *in vitro* cells derived from either WT, AcPb KO, or AcP KO mice. Both doses of IL1 enhanced APs/s and delta wave power in WT cells but not in AcP KO or AcPb KO cells (Fig. 3A and D); these results were anticipated because WT cells have all the AcP isoforms and thus can respond to IL1. The lack of responses in AcPb KO cells suggest that IL1-induced effects on APs and

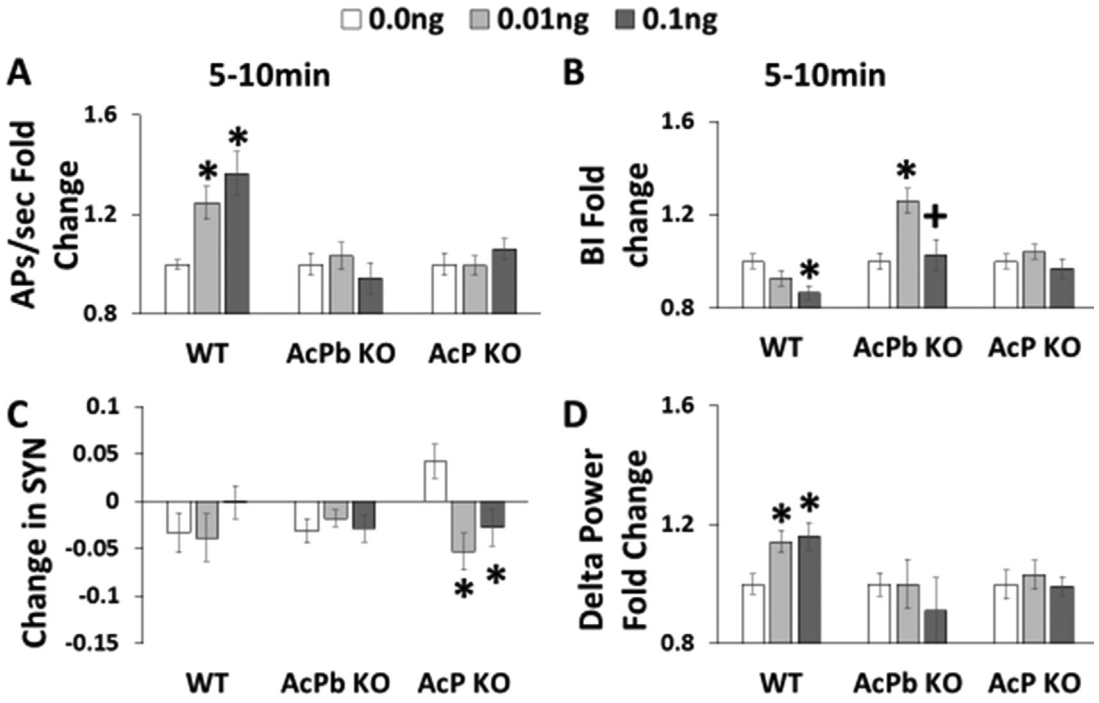

Fig. 3. Interleukin-1β (IL1) altered APs/sec, BI, SYN values, and delta wave power. The means ± SEM values for APs/sec, BI, and delta power were calculated using experimental values from the 5–10 min block intervals after the addition of IL1 and dividing by the baseline, then normalizing to respective MEA 0.0 ng well averages. Change in SYN was calculated by subtracting baseline from experimental values from the same time block. Fig. 2 A, B, D share the same n values: WT - 0.0 ng, n = 79 electrodes; 0.01 ng, n = 79 electrodes; 0.1 ng, n = 81 electrodes; AcPb KO - 0.0 ng, n = 50 electrodes; 0.01 ng, n = 53 electrodes; 0.1 ng, n = 53 electrodes; AcP KO - 0.0 ng, n = 69 electrodes; 0.01 ng, n = 61 electrodes; 0.1 ng, n = 63 electrodes. A) APs/sec values from 3 different doses of IL1. B) BI values from 3 different doses of IL1. C) SYN values from 3 different doses of IL1 (WT - 0.0 ng, n = 170 electrode correlation pairs; 0.01 ng, n = 208 electrode correlation pairs; 0.1 ng, n = 240 electrode correlation pairs; AcPb KO - 0.0 ng, n = 106 electrode correlation pairs; 0.01 ng, n = 157 electrode correlation pairs; 0.1 ng, n = 155 electrode correlation pairs; AcP KO - 0.0 ng, n = 147 electrode correlation pairs; 0.01 ng, n = 191 electrode correlation pairs; 0.1 ng, n = 210 electrode correlation pairs). D) delta wave power (μV^2) values from 3 different doses. Symbols correspond to p- values: * significant difference compared to 0.0 ng value = $p < 0.01$; + significant difference compared between 0.01 ng and 0.1 ng = $p < 0.01$.

delta wave power are mediated by the neuron-specific isoform AcPb. In contrast, the high dose of IL1 reduced the BI in WT cells where as in cells lacking AcPb the low dose enhanced the BI suggesting that isoform AcP, which is present in AcPb KO cells, can enhance the BI in the absence of AcPb. IL1 failed to affect the BI in AcP KO cells (Fig. 3B). SYN was not affected by IL1 in WT cells or in AcPb KO cells (Fig. 3C). In contrast, IL1 lowered SYN values relative to the control 0.0 IL1 values in AcP KO cells. However, the biological significance of the latter result is questioned because differences were dependent upon an elevated SYN response in the control wells and AcP KO cells lack all isoforms of AcP. One way ANOVA analyses (dose) for the 5–10 min time block were: APs (WT - $F_{(2,236)} = 8.112$, $p = 0.0004$; AcPb KO - $F_{(2,153)} = 0.730$, $p = 0.483$; AcP KO – $F_{(2,190)} = 0.768$, $p = 0.465$), BI (WT - $F_{(2,236)} = 4.456$, $p = 0.013$; AcPb KO – $F_{(2,153)} = 7.296$, $p = 0.0001$; AcP KO - $F_{(2,190)} = 1.064$, $p = 0.347$), SYN (WT - $F_{(2,615)} = 1.012$, $p = 0.364$; AcPb KO – $F_{(2,415)} = 0.339$, $p = 0.7128$; AcP KO – $F_{(2,545)} = 6.0020$, $p = 0.003$), delta wave power (WT – $F_{(2,236)} = 5.033$, $p = 0.007$; AcPb KO – $F_{(2,153)} = 0.3645$, $p = 0.695$; AcP KO $F_{(2,190)} = 0.210$, $p = 0.811$). Post-hoc test results for each of the parameters are shown in Fig. 3 as discussed in this paragraph.

3.3. Experiment 3: development of evoked response potential properties

The time course of development of evoked response potentials was determined for WT, AcPb KO, and AcP KO mice-derived cells. The mean peak-to-peak voltage and slow-wave power, the fractions of ERPs whose peak-to-peak voltages exceed a threshold of 10 mV (herein called the high-amplitude fraction), and the fractions of evoked potentials whose slow-wave-power exceed a threshold of 80 dB (called the high-power fraction) are shown in Fig. 5 for each strain, for three development days

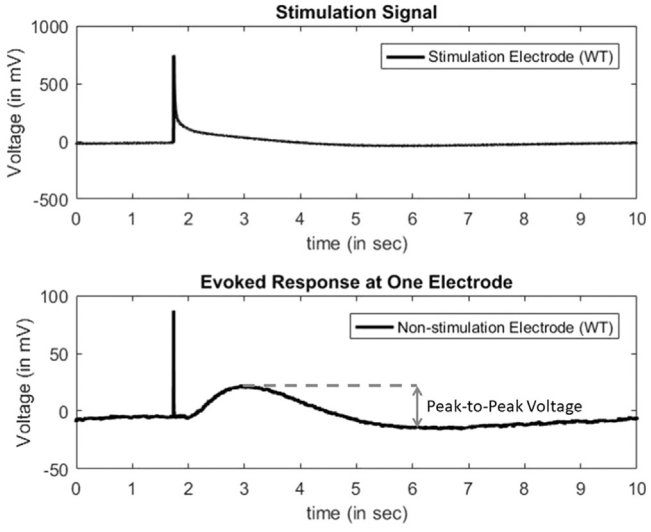

Fig. 4. A typical evoked response in WT cultures. The top plot shows one stimulus which is applied at ~1.8 s. The bottom plot shows the corresponding evoked response potential measured at one non-stimulation electrode. The peak-to-peak voltage of this evoked response potential is also indicated in the plot.

(Day 5, Day 10, and Day 14). (Fig. 4).

Two-way ANOVAs were conducted to determine the dependence of the four ERP properties on development day and strain. Main effects and interaction between the two regressors was considered in the two-way ANOVA. The two-way ANOVAs indicate statistically significant

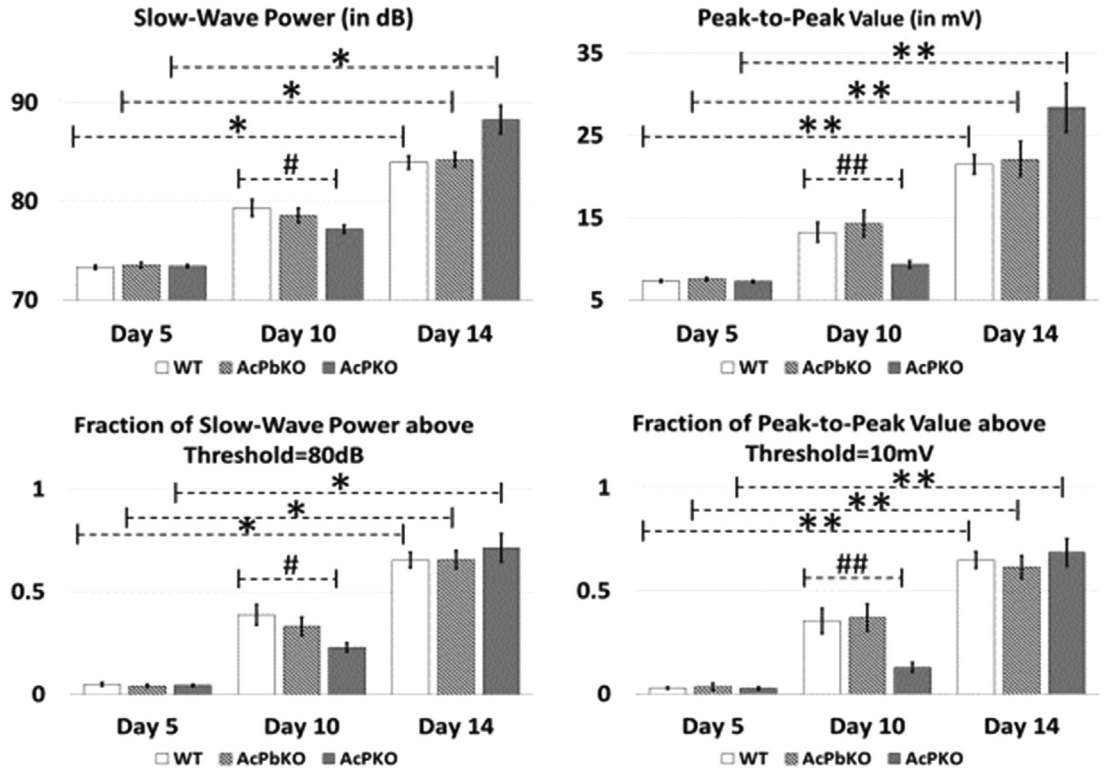

Fig. 5. The means ± standard errors for slow-wave power, peak-to-peak voltages, the fraction of evoked response potentials with slow-wave power exceeding a threshold, and the fraction with peak-to-peak voltages exceeding a threshold, are shown for development days Day 5, Day 10, and Day 14, for the three strains (n = 9 wells for WT and AcPb KO, n = 18 for AcP KO). All four properties show a statistically significant dependence on: the development day for each strain, the strain for development day Day 10, and on the strain-day correlation. The p values from one-way ANOVA analysis are: 1) for the top two figures: * development day = $p < 0.001$; # strain on Day 10 = $p < 0.004$; ** development day = $p < 0.001$; ## strain on Day 10 = $p < 0.001$; 2) for the bottom two figures: * development day = $p < 0.001$; # strain on Day 10 = $p < 0.002$; ** development day = $p < 0.001$; ## strain on Day 10 = $p < 0.001$.

dependence of all four ERP properties (mean peak-to-peak voltage, mean slow-wave power, high-amplitude fraction, high-power fraction) on the development day (for each property, $p < 0.001$ for the main effect of development day). To further examine this dependence, one-way ANOVAs for each ERP property with respect to the development day were conducted, for each individual strain. For all four properties, the one-way ANOVAs showed a statistically-significant dependence on the development day for each strain, specifically: peak-to-peak voltage:$p < 0.001$ for all three strains; slow-wave power:$p < 0.001$ for all three strains; high-amplitude fraction: $p < 0.001$ for all three strains; high-power fraction: $p < 0.001$ for all three strains. All four properties amplify with development day, for each strain.

The two-way ANOVAs do not indicate a statistically dependence of any of the ERP properties on the strain (for each property, $p > 0.1$ for the main effect of strain). However, for each ERP property, the interaction parameter in the two-way ANOVA exhibits statistical significance (peak-to-peak voltage:$p = 0.009$, slow-wave power:$p = 0.02$, high-amplitude fraction: $p = 0.006$; high-power fraction: $p = 0.11$). The two-way ANOVA thus suggests that ERP properties in the main do not have a statistical dependence on the strain, however there should be a dependence for some development days since an interaction is noted. To examine this, one-way ANOVAs were conducted for each ERP property with respect to the strain, for each development day. For Day 5 and Day 14, the four ERP properties do not show a statistically significant dependence with respect to strain (i.e. $p > 0.1$ for each case). However, for Day 10, the four ERP properties each show a statistically significant dependence on the strain (peak-to-peak voltage: $p < 0.001$; slow-wave power: $p < 0.004$; high-amplitude fraction: $p < 0.001$; high-power fraction: $p < 0.002$). It is seen that, on Day 10, the four properties are depressed for AcP KO in comparison to WT and AcPb KO cells; the decrease was most pronounced, in an absolute sense, for the high amplitude and high power fraction.

In sum, the data analyses for Experiment 3 demonstrate that ERPs amplify during cell culture development, regardless of strain. Further, in the main the ERPs have similar characteristics for the three strains. However, the time course of ERP development is slower for AcP KO cells as compared to WT and AcPb KO cells, as indicated by a pronounced depression in the four ERP properties on Day 10 for AcP KO as compared to WT and AcPb KO cells.

4. Discussion

An important finding reported herein is that the absence of AcP isoforms alters the rate of development of electrophysiological emergent network properties. Previously we described BI, SYN, and delta wave power developmental data for WT cells; current results are consistent with those data (Jewett et al., 2015). However, when only AcP is present (in AcPb KO cells), the BI, SYN, and delta wave power rates of development are slower. In contrast, when both AcP and AcPb are absent (AcP KO cells) development rates for the emergent properties are faster (Fig. 2). Results obtained from cells lacking isoforms of AcP are consistent with prior studies suggesting a role for IL1 in brain development e.g. IL1 is highly expressed in the developing brain (Bilbo and Schwarz, 2012) and is critical in developmental processes such as neuron migration (Ma et al., 2014) and survival (Gosselin et al., 2013). Further, IL1 and related cytokines have many neuroendocrine and immune functions in health and disease states. Those interactions have long-term consequences for cognition and other neural functions (Bilbo and Schwarz, 2012). It seems likely, albeit speculative, that the alterations in network emergence of electrophysiological properties occurring in the absence of AcP isoforms (Fig. 2) are related. Thus, adult mice lacking AcPb have little NREMS rebound following sleep loss

(Davis et al., 2015). Further, WT mice upregulate AcPb mRNA, but not AcP mRNA, after sleep loss and the AcPb KO adult mice have exaggerated responses to inflammatory challenges such as lipopolysaccharide (Taishi et al., 2012). Such findings indicate a role for IL1 in brain development; the *in vitro* system used herein provides a way to investigate gene dependency of emergent network properties.

A second important finding is that without AcP and AcPb, i.e. AcP KO cells, or the absence of AcPb alone (i.e. AcPb KO cells), the responsiveness of cells to exogenous IL1 changes. Our interest in the four emergent network properties stems from our prior sleep research. Thus, each of the measures is associated with sleep. During sleep, cortical action potentials (APs/sec) are reduced compared to the waking cortex (Vyazovskiy et al., 2009). During sleep, cortical neurons typically exhibit a burst pause firing pattern with bursts of action potentials occurring for about 500 ms followed by pauses in firing lasting about 500 ms; that pattern along with local network synchronization is associated with slow (< 1.0 Hz) local cortical field potentials during NREMS (McGinty and Szymusiak, 2017; Hajnik et al., 2013). The neuronal/glial tissue culture's spontaneous activity is characterized by bursts and this default firing pattern is thus thought to represent a sleep-like state (Corner, 2008; Hinard et al., 2012; Jewett et al., 2015). *In vivo* delta wave power is posited to reflect the depth of sleep (Davis et al., 2011); cultures can be driven into a deeper sleep-like state by tumor necrosis factor alpha (TNF) as indicated by higher delta wave power values (Jewett et al., 2015). Similarly, in WT cells the higher dose of IL1 enhanced delta wave power suggesting a deeper sleep-like state. However, sleep is also associated with greater EEG synchronization. While the SYN values we calculate are related to EEG synchronization, they are distinct. The effects of IL1 on SYN in cultures of WT cells was minimal.

Although the mechanisms responsible for the differential actions of low and high IL1 doses on the BI in AcPb KO vs WT cells remain unknown (Fig. 3B), it seems likely that they involve IL1-dependent phosphorylation of Src and p38 MAPK. IL1 signals through its type 1 receptor (IL1R). IL1R is found in neurons and astrocytes and both cells mediate IL1- altered sleep (Ingiosi et al., 2015). The IL1/IL1R complex requires an accessory protein (AcP) to signal (Smith et al., 2009). In neurons, there is an alternatively processed form of AcP, AcPb. AcP and AcPb share some signaling events. Of importance to this report, low doses of IL1 enhance Src phosphorylation in neurons, via AcPb (Huang et al., 2011). The IL1 dose needed in hippocampal neurons to phosphorylate Src is about 1000-fold less than needed to activate inflammatory responses (Huang et al., 2011). This observation may be related to the well-known observations that low doses of IL1 may have opposite effects than higher doses. For example, low doses of IL1 promote sleep while higher doses inhibit sleep (Opp et al., 1991). Src family kinases have multiple actions in brain including; regulation of excitatory and inhibitory transmission, learning, memory, depressive behavior, and responses to alcohol (Ohnishi et al., 2011); these processes affect sleep.

IL1 also signals via p38 MAPK phosphorylation and those actions take place in both neurons and astrocytes with the involvement of AcP and to a lesser extent AcPb (Huang et al., 2011). An additional IL1-signalling mechanism involves nuclear factor kappa B/inhibitory kappa B (NFkB/IκB) and they have roles in sleep regulation (Brandt et al., 2004; Chen et al., 1999). However, although AcPb has a modulatory role in p38 MAPK phosphorylation, it lacks signaling via NFkB. Regardless, IL1, also promotes transcription of receptor mRNAs such as the adenosine A1 receptor and the glutamate AMPA receptor-gluR1 via NFkB (Krueger, 2008; Krueger et al., 2013; Krueger et al., 2008). These receptors are involved in sleep.

There is also a soluble isoform of AcP, (sAcP). Like AcPb, sAcP is anti-inflammatory (Smith et al., 2009; Taishi et al., 2012). However, sAcP binds to the type 2 IL1 receptor thereby increasing its affinity to IL1 about 100-fold; such an action would effectively reduce extracellular IL1 access to the type 1 IL1 receptor (Smith et al., 2003). Interestingly, AcPb KO mice express higher amounts of sAcP mRNA in the somatosensory cortex than WT mice, perhaps as a compensatory mechanism for the loss of anti-inflammatory AcPb (unpublished data). How these various mechanisms interact to change the sensitivities of the AcP KO and AcPb KO cells (Fig. 3) remains unknown although the lack of AcP isoforms affects cell sensitivity to IL1.

Peak-to-peak voltage and slow-wave power (top two figures in Fig. 5) are metrics that correlate with well-formed evoked response potentials in connected neuronal networks (Rector et al., 2005, 2009). The analyses here indicate well-formed ERPs develop with time in neuronal networks cultured from cells derived from WT, AcPb KO, and AcP KO one-to-two day-old mice. The *in vitro* ERP emergence is indicated both in the amplification in the mean peak-to-peak voltage and slow-wave power, and in the fractions of the evoked potentials where these metrics exceed a threshold (i.e., high-amplitude fraction and high power fraction) (bottom two figures in Fig. 5). These properties show no dependence on strain on days 5 and 14, but are reduced in AcP KO cultures on day 10 compared to the WT, indicating a slower development of well-formed evoked potentials in AcP KO cells. Although speculative, this indicates that AcP is required for the timely development of ERPs, but that cells lacking AcP acclimate to the loss within two weeks of culture. Because the high-amplitude fraction and high-power fraction amplify markedly with development day, we speculate that development is reflected by an increasing prevalence of well-formed evoked potentials rather than a gradual amplification of all evoked potentials.

The direct electrically stimulated ERPs observed in cultured cells are however, greater in amplitude, slower in onset, and longer in duration than corresponding ERPs induced by activation of afferent neurons *in vivo* (Rector et al., 2005, 2009). Although the reasons for this were not studied herein, it seems likely that differences such as the non-specific activation of many cells by electrical stimulation *in vitro*, the dramatically different *in vivo* vs *in vitro* topological structures and network connectivity, the lack of blood flow *in vitro*, and the different analytical techniques used to derive ERPs (e.g. *in vivo* multiple ERPs are signal averaged whereas this is not necessary *in vitro* due to their larger amplitudes and more consistent time course), all contribute to the observed differences. Of importance is that IL1/AcP contributes to evoked response ontology as well as many other emergent network properties and this likely has many manifestions in brain development. The cell culture system described herein coupled with the use of mutant cells provides an experimental platform to examine brain development gene dependencies (Lu et al., 2016).

The emergent properties characterized herein are also used *in vivo* to define sleep and wake states. We and others have argued that the small networks in culture exhibit sleep- and wake-like states with the sleep-like state being the default state in culture due to its burstiness nature (Corner, 2008; Hinard et al., 2012; Jewett et al., 2015). Like animals, cultures respond to chemical stimulation, whether wake- (Hinard et al., 2012; Corner, 2008) or sleep-inducing (Jewett et al., 2015 and Fig. 2), cultures exhibit sleep homeostasis (Jewett et al., 2015; Saberi-Moghadam et al., 2018), and gene expression profiles in cultured networks parallel those of the waking/sleeping brain (Hinard et al., 2012). Furthermore, small networks *in vivo*, e.g. cortical columns, can oscillate between sleep- and wake-like states as characterized via the amplitudes of the ERPs. The cortical column sleep-like state also exhibits sleep homeostasis (Rector et al., 2005). Individual cortical column state is also linked to animal behavior. Thus, if rats were trained to lick a sweet solution when a specific facial whisker was stimulated, when the column was in a sleep-like state as evidenced by high ERP amplitudes (while the rat was awake and behaving), the rat made errors of omission and commission. In contrast, if the column was in the wake-like state (exhibiting low amplitude ERPs) the rats did not make mistakes (Krueger et al., 2013). Those data coupled with other observations suggesting that parts of the brain can be awake while simultaneously other parts can be asleep (Krueger et al., 2013; Krueger and Roy, 2016)

along with the current data support the hypothesis that sleep-like states are a fundamental property of any viable small network whether *in vivo* or *in vitro*.

Acknowledgements

Supported by grants to JMK from the National Institutes of Health (USA grant numbers NS025378 and NS096259) and by grants to SR from the United States National Science Foundation (grant numbers CNS1545104 and CMMI1635184).

Data Accessibility

Data files, spreadsheets, data analyses programs, and codes used to generate data and figures will be made available upon further request to the corresponding author.

Conflict of interest

None.

References

Bellinger, F.P., Madamba, S., Siggins, G.R., 1993. Interleukin 1 beta inhibits synaptic strength and long-term potentiation in the rat CA1 hippocampus. Brain Res. 628, 227–234.
Bilbo, S.D., Schwarz, J.M., 2012. The immune system and developmental programming of brain and behavior. Front. Neuroendocrinol. 33, 267–286.
Boraschi, D., Tagliabue, A., 2013. The interleukin-1 receptor family. Semin. Immunol. 25, 394–407.
Brandt, J.A., Churchill, L., Rehman, A., Ellis, G., Mémet, S., Israël, A., Krueger, J.M., 2004. Sleep-deprivation increases activation of nuclear factor kappa B in lateral hypothalamic cells. Brain Res. 1004, 91–97.
Chen, Z., Gardi, J., Kushikata, T., Fang, J., Krueger, J.M., 1999. Nuclear factor kappa B-like activity increases in murine cerebral cortex after sleep deprivation. Am. J. Physiol. 45, R1812–R1818.
Corner, M.A., 2008. Spontaneous neuronal burst discharges as dependent and independent variables in the maturation of cerebral cortex tissue cultured in vitro: a review of activity-dependent studies in live 'model' systems for the development of intrinsically generated bioelectric slow-wave sleep patterns. Brain Res. Rev. 59, 221–244.
Cullinan, E.B., Kwee, L., Nunes, P., Shuster, D.J., Ju, G., McIntyre, K.W., Chizzonite, R.A., Labow, M.A., 1998. IL-1 receptor accessory protein is an essential component of the IL-1 receptor. J. Immunol. 161, 5614–5620.
Dinarello, C.A., 2009. Immunological and inflammatory function of the interleukin-1 family. Annu. Rev. Immunol. 27, 519–550.
Davis, C.J., Clinton, J.M., Jewett, K., Zielinski, M.R., Krueger, J.M., 2011. EEG delta wave power: an independent sleep phenotype or epiphenomena? J. Clin. Sleep Med. 7, S16–S18.
Davis, C.J., Dunbrasky, D., Oonk, M., Taishi, P., Opp, M.R., Krueger, J.M., 2015. The neuron-specific interleukin-1 receptor accessory protein is required for homeostatic sleep and sleep responses to influenza viral challenge in mice. Brain Behav. Immun. 47, 35–43.
De, A., Churchill, L., Obál Jr., F., Simasko, S.M., Krueger, J.M., 2002. GHRH and IL1β increase cytoplasmic Ca^{2+} levels in cultured hypothalamic GABAergic neurons. Brain Res. 949, 209–212.
Gardoni, F., Boraso, M., Zianni, E., Corsini, E., Galli, C.L., Cattabeni, F., Marinovich, M., Di Luca, M., Viviani, B., 2011. Distribution of interleukin-1 receptor complex at the synaptic membrane driven by interleukin-1β and NMDA stimulation. J. Neuroinflammation 8, 1–6.
Garlanda, C., Dinarello, C.A., Mantovani, A., 2013. The interleukin-1 family: back to the future. Immunity 39, 1003–1018.
Goshen, I., Yirmiya, R., 2009. Interleukin-1 (IL-1): a central regulator of stress responses. Front. Neuroendocrinol. 30, 30–45.
Gosselin, D., Bellavance, M.A., Rivest, S., 2013. IL-1RAcPb signaling regulates adaptive mechanisms in neurons that promote their long-term survival following excitotoxic insults. Front. Cell Neurosci. 7, 1–12.
Gruber-Schoffnegger, D., Drdla-Schutting, R., Honigsperger, C., Wunderbaldinger, G., Gassner, M., Sandkuhler, J., 2013. Induction of thermal hyperalgesia and synaptic long-term potentiation in the spinal cord lamina I by TNF-α and IL-1β is mediated by glia cells. J. Neurosci. 33, 6540–6551.
Hajnik, T., Toth, A., Detari, L., 2013. Characteristic changes in cortical waves after 6-h sleep deprivation in rat. Brain Res. 1501, 1–11.
Hinard, V., Mikhail, C., Pradervand, S., Curie, T., Houtkooper, R.H., Auwerx, J., Franken, P., Tafti, M., 2012. Key electrophysiological, molecular, and metabolic signatures of sleep and wakefulness revealed in primary cortical cultures. J. Neurosci. 32, 12506–12517.
Huang, Y., Smith, D.E., Ibanez-Sandoval, O., Sims, J.E., Friedman, W.J., 2011. Neuron-specific effects of interleukin-1β are mediated by a novel isoformof the IL-1 receptor accessory protein. J. Neurosci. 31, 8048–18059.
Imeri, L., Opp, M.R., 2009. How (and why) the immune system makes us sleep. Nat. Rev. Neurosci. 10, 199–210.
Ingiosi, A.M., Raymond Jr., R.M., Pavlova, M.N., Opp, M.R., 2015. Selective contributions of neuronal and astroglial interleukin-1 receptor 1 to the regulation of sleep. Brain Behav. Immun. 48, 244–257.
Jewett, K.A., Krueger, J.M., 2012. Humoral sleep regulation; interleukin-1 and tumor necrosis factor. Vitam. Horm. 89, 241–257.
Jewett, K.A., Taishi, P., Sengupta, P., Roy, S., Davis, C.J., Krueger, J.M., 2015. Tumor necrosis factor enhances the sleep-like state and electrical stimulation induces a wake-like state in co-cultures of neurons and glia. Eur. J. Neurosci. 42, 2078–2090.
Jimbo, Y., Robinson, H.P., Kawana, A., 1998. Strengthening of synchronized activity by tetanic stimulation in cortical cultures; application of planar electrode arrays. IEEE Trans. Sio-Med. Eng. 45, 1297–1304.
Katsuki, H., Nakai, S., Hirai, Y., Akaji, K., Kiso, Y., Satoh, M., 1990. Interleukin-1 beta inhibits long-term potentiation in the CA3 region of mouse hippocampal slices. Eur. J. Pharmacol. 181, 323–326.
Kawasaki, Y., Zhang, L., Cheng, J.K., Ji, R.R., 2008. Cytokine mechanisms of central sensitization: distinct and overlapping role of interleukin-1β, Interleukin-6 and tumor necrosis factor-α in regulating synaptic and neuronal activity in the superficial spinal cord. J. Neurosci. 28, 5189–5194.
Krueger, J.M., Walter, J., Dinarello, C.A., Wolff, S.M., Chedid, L., 1984. Sleep-promoting effects of endogenous pyrogen (interleukin-1). Am. J. Physiol. 246, R994–R999.
Krueger, J.M., Obál Jr., F., 1993. A neuronal group theory of sleep function. J. Sleep Res. 2, 63–69.
Krueger, J.M., 2008. The role of cytokines in sleep regulation. Curr. Pharm. Des. 14, 3408–3416.
Krueger, J.M., Rector, D.M., Roy, S., Van Dongen, H.P., Belenky, G., Panksepp, J., 2008. Sleep as a fundamental property of neuronal assemblies. Nat. Rev. Neurosci. 9, 910–919.
Krueger, J.M., Huang, Y., Rector, D.M., Buysee, D.J., 2013. Sleep: a synchrony of cell activity-driven small network states. Eur. J. Neurosci. 38, 2199–2209.
Krueger, J.M., Frank, M., Wisor, J., Roy, S., 2016. Sleep function: toward elucidating an enigma. Sleep. Med. Rev. 28, 42–50.
Krueger, J.M., Roy, S., 2016. Sleep's kernel. Scientist 30, 36–41.
Lu, C., Chen, Q., Zhou, T., Bozic, D., Fu, Z., Pan, J.Q., Feng, G., 2016. Micro-electrode array recordings reveal reductions in both excitation and inhibition in cultured cortical neuron networks lacking Shank3. Mol. Psychiatry 21, 159–168.
Ma, L., Li, X.W., Zhang, S.J., Yang, F., Zhu, G.M., Yuan, X.B., Jiang, W., 2014. Interleukin-1 beta guides the migration of cortical neurons. J. Neuroinflammation 11, 114–124.
McGinty, D., Szymusiak, Rl, 2017. Neural control of sleep in mammals. In: Kryger, Toth, Dement (Eds.), Principles and Practice of Sleep Medicine. Elsevier, pp. 62–77.
Ohnishi, H., Murata, Y., Okazawa, H., Matozake, T., 2011. Src family kinases: modulators of neurotransmitter receptor function and behavior. Trends Neurosci. 34, 629–637.
Opp, M.R., Obál Jr., F., Krueger, J.M., 1991. Interleukin-1 alters rat sleep: temporal and dose-related effects. Am. J. Physiol. 260, R52–R58.
Prieto, G.A., Snigdha, S., Baglietto-Vargas, D., Smith, E.D., Berchtold, N.C., Tong, L., Ajami, D., LaFerla, F.M., Rebek Jr., J., Cotman, C.W., 2015. Synapse-specific IL-1 receptor subunit reconfiguration augments vulnerability to IL-1β in the aged hippocampus. Proc. Natl. Acad. Sci. USA 112, E5078–E5087.
Rector, D.M., Topchiy, I.A., Carter, K.M., Rojas, M.J., 2005. Local functional state differences between rat cortical columns. Brain Res. 1047, 45–55.
Rector, D.M., Schei, J.L., Van Dongen, H.P., Belenky, G., Krueger, J.M., 2009. Physiological markers of local sleep. Eur. J. Neurosci. 29, 1771–1778.
Roy, S., Krueger, J.M., Rector, D.M., Wan, Y., 2008. Network models for activity-dependent sleep regulation. J. Theor. Biol. 253, 462–468.
Saberi-Moghadam, S., Simi, A., Setareh, H., Mikhail, C., Tafti, M., 2018. In vitro cortical network firing is homeostatically regulated: a model for sleep regulation. Sci. Rep. 8, 6297–6310.
Smith, D.E., Hanna, R., Della, F., Moore, H., Chen, H., Farese, A.M., MacVittie, T.J., Virca, G.D., Sims, J.E., 2003. The soluble form of IL-1 receptor accessory protein enhances the ability of soluble type II IL-1 receptor to inhibit IL-1 action. Immunity 18, 87–96.
Smith, D.E., Lipsky, B.P., Russell, C., Ketchem, R.R., Kirchner, J., Hensley, K., Huang, Y., Friedman, W.J., Boissonneault, V., Plante, M.M., Rivest, S., Sims, J.E., 2009. A central nervous system-restricted isoform of the interleukin-1 receptor accessory protein modulates neuronal responses to interleukin-1. Immunity 30, 817–831.
Taishi, P., Davis, C.J., Bayomy, O., Zielinski, M.R., Liao, F., Clinton, J.M., Smith, D.E., Krueger, J.M., 2012. Brain –specific interleukin-1 receptor accessory protein in sleep regulation. J. Appl. Physiol. 112, 1015–1022.
Vyazovskiy, V.V., Olcese, U., Lazimy, Y.M., Faraguna, U., Esser, S.K., Williams, J.C., Cirelli, C., Tononi, G., 2009. Cortical firing and sleep homeostasis. Neuron 63, 865–878.
Yirmiya, R., Goshen, I., 2011. Immune modulation of learning, memory, neural plasticity and neurogenesis. Brain Behav. Immun. 25, 181–213.
Wagenaar, D.A., Madhavan, R., Pine, J., Potter, S.M., 2005. Controlling bursting in cortical cultures with closed-loop multi-electrode stimulation. J. Neurosci. 25, 680–688.
Yoshida, T., Shiroshima, T., Le, S.J., Yasumura, M., Uemura, T., Chen, X., Iwakura, Y., Mishina, M., 2012. Interleukin-1 receptor accessory protein organizes neuronal synaptogensesis as a cell adhesion molecule. J. Neurosci. 32, 2588–2600.